

UCSF

UC San Francisco Previously Published Works

Title

Androgen Receptor Upregulation Mediates Radioresistance after Ionizing Radiation

Permalink

<https://escholarship.org/uc/item/8tt7p4sh>

Journal

Cancer Research, 75(22)

ISSN

0008-5472

Authors

Spratt, Daniel E
Evans, Michael J
Davis, Brian J
[et al.](#)

Publication Date

2015-11-15

DOI

10.1158/0008-5472.can-15-0892

Peer reviewed



Published in final edited form as:

Cancer Res. 2015 November 15; 75(22): 4688–4696. doi:10.1158/0008-5472.CAN-15-0892.

Androgen receptor upregulation mediates radioresistance after ionizing radiation

Daniel E. Spratt^{1,2,3}, Michael J. Evans², Brian J. Davis⁴, Michael G. Doran³, Man Xia Lee², Neel Shah², John Wongvipat², Kathryn E. Carnazza³, George G. Klee⁵, William Polkinghorn^{1,2}, Donald J. Tindall⁵, Jason S. Lewis^{3,#}, and Charles L. Sawyers^{2,#}

¹Department of Radiation Oncology, Memorial Sloan Kettering Cancer Center

²Human Oncology Pathogenesis Program, Memorial Sloan Kettering Cancer Center

³Department of Radiology and Molecular the Molecular Pharmacology & Chemistry Program, Memorial Sloan Kettering Cancer Center

⁴Department of Radiation Oncology, Mayo Clinic Rochester

⁵Departments of Urology and Biochemistry/Molecular Biology, Mayo Clinic

Abstract

Clinical trials have established the benefit of androgen deprivation therapy (ADT) combined with radiotherapy (RT) in prostate cancer. ADT sensitizes prostate cancer to RT-induced death at least in part through inhibition of DNA repair machinery, but for unknown reasons adjuvant ADT provides further survival benefits. Here we show that androgen receptor (AR) expression and activity are durably upregulated following RT in multiple human prostate cancer models *in vitro* and *in vivo*. Moreover, the degree of AR upregulation correlates with survival *in vitro* and time to tumor progression in animal models. We also provide evidence of AR pathway upregulation, measured by a rise in serum levels of AR-regulated hK2 protein, in nearly 20 percent of patients after RT. Furthermore, these men were three fold more likely to experience subsequent biochemical failure. Collectively, these data demonstrate that RT can upregulate AR signaling post-therapy to an extent that negatively impacts disease progression and/or survival.

Keywords

radiotherapy; prostate cancer; androgen receptor; radioresistance; DNA repair

INTRODUCTION

Several phase III clinical trials have demonstrated a clear survival benefit when long term adjuvant androgen deprivation therapy (LTADT) is added to concurrent ADT and external

[#]Corresponding author (co-corresponding): Jason S. Lewis, Radiochemistry & Imaging Sciences Service, Department of Radiology, Memorial Sloan Kettering Cancer Center, 1275 York Avenue, New York, NY 10065. Phone: 646-888-3038; Fax: 646-422-0408; lewisj2@mskcc.org. Charles L. Sawyers, Human Oncology and Pathogenesis Program, Memorial Sloan Kettering Cancer Center, 1275 York Avenue, New York, NY 10065. Phone: 646-888-2594; Fax: 646-888-2595, sawyersc@mskcc.org.

Conflicts of interest: CLS and JW are co-inventors of MDV3100. DJT and GGK hold patents for the immunoassay of hK2.

beam radiotherapy (RT) (1,2). The addition of adjuvant ADT post RT is commonly referred to as LTADT, however recent evidence suggests that simply increasing duration of ADT without the focus on when it is given in relation to RT does not improve outcomes, suggesting the timing and duration of ADT is critical (3). However, chronic androgen suppression can impact quality of life, motivating ongoing clinical studies to optimize the duration of androgen deprivation without compromising efficacy (3,4).

We previously have shown that primary prostate tumors display heterogeneity in AR transcriptional output, which could result in differential sensitivity to ADT and to the relative clinical benefit of ADT when combined with RT (5). Furthermore, we and others have also shown that AR activates DNA repair pathways, providing further rationale for concurrent ADT/RT therapy (5–7). Despite this radiosensitizing mechanistic action of ADT, clinical trials have demonstrated that adjuvant ADT has similar efficacy to that of concurrent ADT with RT,(8) begging the question why adjuvant ADT sufficiently compensates for radiosensitizing concurrent therapy, and further improves survival even beyond concurrent use of ADT with RT (1).

In addition to variability in baseline AR signaling, select observations may suggest that AR signaling is upregulated by RT. For instance, in small patient series a subset of patients have increases in secreted levels of AR target genes (e.g. PSA, hK2) during EBRT (9,10). In addition, the AR target gene TMRSS2 is upregulated in a human prostate cancer cell line exposed to therapeutic doses of RT (6). These considerations led us to more broadly study the impact of RT on AR signaling, and the association between high AR signaling post RT and measures of outcome, as this may have implications for the use and duration of adjuvant ADT post RT.

MATERIALS AND METHODS

Cell lines

LNCaP and MDA-PCa2b cell lines used were purchased directly from American Type Culture Collection (ATCC) (Manassas, VA) and cultured according to recommended specifications. LNCaP-AR is an AR-overexpressing (wild type) cell line originally derived from parental LNCaP with a luciferase probasin reporter. LNCaP-AR cell line was authenticated via AR overexpression by PCR, immunoblot, and luciferase assay. CWR22Pc were obtained from Marja Nevelanan, Thomas Jefferson University.

Cell culture

Cell lines were not kept in culture longer than 6 months. Growth conditions for each cell line are described in the Supplemental methods.

Cell irradiation

All described doses of radiation were delivered using Cesium-137 irradiator (Shepherd Mark, Model 68). Correction factors for decay were implemented and the estimated dose rate of delivered was 184 cGy/min. All plates were continuously rotated with a turntable speed of 6 revolutions/minute to improve dose homogeneity.

Realtime PCR

Cells were plated and 24 hours later irradiated. At the specified time post-RT cells were collected for RNA extraction using the Qiagen kit and RNA-easy kit (QIAGEN, QIA Shredder, #79656, QIAGEN, RNeasy Mini Kit, #74106). cDNA was generated using the Applied biosystems High capacity cDNA Reverse Transcription Kit (#4368814). Per manufacturers recommendations Quantifast (QIAGEN, Quantifast SYBR Green PCR kit, #204057) was used for PCR. All assays were performed in quadruplicate and normalized to actin. PCR primers can be found in Supplementary methods.

Western blot analysis

Whole cell lysates were prepared using 10% M-PER lysis buffer and clarified by centrifugation. Proteins were separated by 4–12% SDS-PAGE 15 well gel as prepared as previously described. Primary antibodies for the following proteins were used: AR (Santa Cruz, AR (N-20), sc-816, 1:500-1000 dilution), Gamma-hk2ax (Millipore, Anti-phospho-Histone H2A.x (ser139), clone JBW301, 05-636, 1:500-1000 dilution), pChk2, (Cell Signaling Technology, p-Chk2 (T68) (C13C1), 2197s, 1:1000 dilution), GAPDH (Abcam, GAPDH, ab9485 (1:10,000)). Secondary antibodies used included Jackson Immuno Research, Goat anti-mouse HRP (115-035-003, 1-10,000 dilution) and Goat anti-rabbit HRP (111-035-003, 1-10,000 dilution).

¹⁸F-FDHT internalization assay

Internalization of ¹⁸F-DHT was investigated on LNCaP cells. Approximately 1×10^5 cells were plated in 12-well plates and incubated overnight, and the next day the plates were irradiated with the specified increasing doses of RT. 24 hours post-RT 2 mL of radiolabeled DHT (37 kBq/mL) was added to each well. The plates were incubated at 37 °C for 1 h. The medium was then collected and the cells were rinsed with 1 mL of PBS twice. Adherent cells were lysed with 1 mL of 1 M NaOH. Each wash was collected, isolated, and counted for activity. For each plate 2 wells were reserved for cell counting in order to normalize uptake per cell. This experiment was conducted in both charcoal-stripped media and full serum.

Neutral Comet assay

LNCaP and LNCaP-AR cells were grown in described conditions above for two days and the neutral Comet assay was performed using CometAssay® Electrophoresis System (CometAssay® 2 Well ES Unit w/ Starter Kit and Power Supply: #4250-050-ESK-PS1) per assay protocol.

Immunofluorescence assays

LNCaP and LNCaP-AR cells were grown as described above in parallel for 24 hours on 4-chamber slides (Thermo Scientific, Lab-Tek II Chamber Slide w/cover CC2 Glass slide sterile, 154917), approximately 125,000 cells/well in 500uL total volume. Following RT using the cell irradiator, cells were washed twice with PBS and fixed with 4% PFA and 0.2% Triton X-100. The primary antibody for AR (Santa Cruz, AR (N-20), sc-816, 1:200 dilution) or gamma-H2aX (Millipore, Anti-phospho-Histone H2A.x (ser139), clone

JBW301, 05-636, 1:200 dilution) incubated overnight at 4 degrees, and then washed followed by incubation with the secondary antibody for AR (Vector Laboratories, DyLight 594, D1-1594, 1:100 dilution) or gamma-H2aX (Invitrogen, Alexa Fluor 488, A11001, 1:500 dilution) for one hour at room temperature, and co-stained for DAPI. Confocal microscopy (LSM 5 LIVE) with a 20X/0.8NA objective and foci were counted using Metamorph image analysis software (Molecular Devices). An average of 1000 distinct nuclei were counted per time point.

Clonogenic assay

LNCaP, LNCaP-AR, and CWR22Pc cells were grown in into 6-well, tissue-culture treated polystyrene plates (BD Falcon) in a series of serial dilutions (24,000, 12,000, 3000, 1000, 333, and 111 cells per well) at each dose. Cells received either 0, 2, 4, or 6 Gy of RT. Plates were incubated for 2 weeks, then washed and fixed with methanol, and stained with 0.2% crystal violet (Sigma) in 10% formalin (Sigma). Plates were scanned and counted by GelCount (Oxford Optronix) and its accompanying software.(5)

Xenografts

All animal studies were conducted in compliance with the Research Animal Resource Center guidelines at our institution. Approximately five week old male CB-17 SCID mice were obtained from Taconic Farms (Deerwood, MD). 2×10^6 LNCaP-AR cells were injected subcutaneously into the one (or both) flanks of intact male mice in a 1:1 mixture by volume of Matrigel and media. Experiments were initiated once tumors were palpable, and tumor volume measurements were estimated by hand caliper measurements in three dimensions. Tumors were harvested and analyzed for protein, mRNA, immunofluorescence, or immunohistochemistry.

Bioluminescence *in vivo* assay

AR function was determined *in vivo* by measuring luciferase activity of human LNCaP-AR xenografts grown in male mice. These tumors co-expressed exogenous AR and the AR-dependent reporter construct ARR2-Pb-Luc. D-Luciferin (Perkin Elmer) was dissolved in PBS to 15 mg/mL. Mice were injected with 200 μ l (3 mg) via intraperitoneal injection. Following injection, mice were placed under anesthesia with a mixture of 2.5% isoflurane and oxygen for five minutes. The mice were imaged using the IVIS Spectrum for the duration of 30 seconds. Images were taken at specified time points pre- and post-RT.

Patient serum analysis

Patient serum was collected at the Mayo clinic on an Institutional Review Board–approved study of prospective biomarker collection. Patients enrolled were almost exclusively low and intermediate risk by NCCN criteria. Most patients were treated with EBRT as monotherapy. No patients underwent a radical prostatectomy. Serum specimens were collected, analyzed, and stored at baseline before the initiation of radiotherapy and at the first follow-up visit after treatment (3–7 months post-RT). Both serum PSA and free-PSA were measured utilizing the Hybritech assays on an Access analyzer (Beckman Coulter, Inc). Free-hK2 levels were measured utilizing a selective pair of monoclonal antibodies. The

assay was implemented on the Access analyzer, and the cross-reactivity with PSA is negligible as previously described.(11) The hK2 limit of detection was 1.5 pg/mL and the day-to-day coefficient of variation set at <15%, was <4 pg/mL.

Statistical analyses

All qPCR analyses, IHC comparisons, and comet assay comparisons were performed with a two-sided t-test. Correlation statistics were performed using R-squared statistics. *In vivo* tumor growth comparisons were estimated by actuarial likelihood estimates using the inverse Kaplan-Meier method with log-rank statistics to obtain cumulative incidence rates. Statistical analysis was performed using SPSS version 21 (SPSS, Inc, USA). Patient data statistics were conducted using logistical regression to compare patients with and without a rise in Hk2 post-RT reported as an odds ratio and 95% confidence interval. Kaplan-Meier time point comparisons (72 months) were performed with a Chi-Squared test. Baseline patient group comparison between those with and without Hk2 gain were performed using the Fisher's Exact test or Mantel-Haenszel Chi-Squared test for ordinal and categorical variables, and the Wilcoxon-Mann-Whitney test for continuous variables. For all analyses, two-sided *P* values of .05 were considered statistically significant.

RESULTS

We first tested whether RT had direct biological effects on AR regulation and expression. Four human prostate cancer cell lines (LNCaP, LNCaP-AR, MDA-PCa2b, and CWR22Pc) showed a dose dependent increase in AR mRNA after exposure to 1, 6, and 12 Gy at 24 hours post-RT (Fig 1a). AR protein levels were also upregulated in three (LNCaP, LNCaP-AR, and CWR22Pc) of the four cell lines at the same time points (Fig 1b). AR nuclear protein translocation was also enhanced by RT, as immunofluorescence showed that the overall percentage of nuclear AR, measured 24 hours post-RT, was 25–45% fold higher compared to vehicle control (Supplemental Fig 1a). To provide further evidence of AR protein upregulation, we used a ligand binding assay with ¹⁸F labeled dihydrotestosterone (¹⁸F-FDHT) (Supplemental Fig 1b). When ¹⁸F-FDHT was added to LNCaP cells plated in androgen-free media and irradiated with increasing doses of RT, even at 1 Gy, there was a significant increase in uptake of ¹⁸F-FDHT. This increase is consistent with increased AR protein expression and/or available ligand binding sites, and was abrogated when the experiment was performed in androgen-replete serum (due to competition of unlabeled ligand with ¹⁸F-FDHT).

To test if RT-induced AR upregulation occurs *in vivo*, subcutaneous LNCaP-AR tumors were established in mice and treated with 10 Gy of conformal external beam RT, and harvested at 1, 3, 5, 7, and 9 days post-RT. AR mRNA expression was increased, albeit with heterogeneity across tumors, in 18 of 19 mice compared to the non-irradiated group (*p*<0.05), with some tumors showing large (>15 fold) increases (Fig 1c). AR protein levels increased at 24 hours, peaked at 5 days, and persisted in some tumors for at least 9 days post-RT (Fig 1d).

Next, bilateral LNCaP-AR xenografts were established, and the left flank tumor was treated with 10 Gy (2.5 Gy per field) using a 4-field technique for improved tissue dose

homogeneity (Supplemental Fig 1d). Treatment planning software determined that the contralateral tumor received minimal scatter dose of EBRT (Dmax of 65 cGy), thereby serving as a control. Five days post-RT the tumors were harvested, paraffin embedded, sectioned and assessed for AR expression analysis by immunohistochemistry and immunofluorescence (Fig 1e). To quantify the change in AR intensity, the immunofluorescence slides were digitized, random areas of tumor were captured and approximately 600 cells in the control and RT group were quantified via staining intensity by standard software computation. Mean AR expression was increased compared to non-irradiated tumors ($p < 0.0001$), but with considerable heterogeneity suggesting that a subgroup of cells may be “primed” to respond to RT in this manner (Fig 1e). Collectively, these results show that AR mRNA and protein is acutely upregulated post-EBRT within 24 hours, and is maintained in a heterogeneous manner even after a single fraction of EBRT.

Having demonstrated that RT leads to increased AR expression and nuclear localization *in vitro* and *in vivo*, we asked if downstream AR transcriptional output was altered. Indeed, LNCaP-AR cells treated with increasing dose of RT (0, 1, 6, and 12 Gy) EBRT and harvested 24 hours post treatment showed increased expression of established canonical AR-target genes (KLK2, KLK3, TMPRSS2) (Fig 2a).

TMPRSS2, KLK3 and KLK2 were also upregulated in LNCaP-AR xenografts during the first week after treatment with 10 Gy of conformal EBRT, but this induction was not observed in all mice and the magnitude of induction varied by the target gene analyzed. KLK2 was most the consistently upregulated of the tested target genes (95% of mice experienced an upregulation over untreated controls), while PSA demonstrated an increase in less than half of the mice (47%) and TMPRSS2 was intermediate (73%) (Fig 2b). Because kinetics of AR induction in this model is variable during the first week post-RT, we used the androgen responsive ARR₂Pb-luciferase reporter system in the LNCaP-AR model to perform serial imaging 1, 3, 5, and 7 days post-EBRT. This approach to measure AR pathway activation also revealed heterogeneity in AR induction across the cohort, with 19 of the 25 mice (76%) demonstrating increases in AR-output over baseline at any time during the first week post-RT (Fig 2c). Minor stochastic mutational changes that arise during tumor growth may manifest as larger changes in radiosensitivity as well as AR output.

Given the variable range of AR upregulation post EBRT (either among cell lines *in vitro* or among tumors *in vivo*), we next asked whether these differences correlated with tumor cell survival. We first performed a clonogenic survival assay with the isogenic cell line panel, LNCaP and LNCaP-AR, and with CWR22Pc, which has relatively low baseline AR expression but large induction of AR mRNA post EBRT (Fig 3a). Of note, the magnitude of AR upregulation was more highly correlated with the surviving fraction ($p < 0.005$, Fig 3b) than the baseline AR level. This finding is consistent with more direct assessments of RT-induced DNA damage by neutral comet assay (Fig 3c) and by gamma-H2AX induction by immunofluorescence (Fig 3d) or western blot (Supplemental Fig 2a), all of which show more rapid resolution of DNA damage in LNCaP-AR compared to parental LNCaP.

To study the impact of AR induction on survival *in vivo*, we treated a cohort of mice bearing subcutaneous LNCaP-AR xenografts with 10 Gy of EBRT. We tracked AR induction by

bioluminescence (as in Fig 2c) and monitored tumor volume changes over four weeks (Fig 3e). The maximum percent change in bioluminescence during the first week post-RT was significantly correlated with time to tumor progression (R^2 0.77, $p < 0.0001$). Furthermore, time to progression in tumors with the largest increase in AR-output post-EBRT (>50%) was significantly shorter than those with a modest increase (0–50%) or a decline in AR output ($p < 0.001$, Fig 3f). Of note, pre-treatment tumor bioluminescence signal did not correlate with time to tumor progression (Supplemental Fig 2b), consistent with the results from our *in vitro* data showing that post-RT AR induction was more highly correlated with radioresistance than baseline AR levels (Fig 3d).

Lastly, we asked if there is any clinical evidence of post-RT changes in AR-output and whether these changes correlate with clinical outcome in a cohort of 227 men with predominantly low and intermediate risk prostate cancer who were enrolled in a prospective trial to collect baseline and serial serum free-Hk2 (KLK2) measurements post-RT. All of these men had evaluable baseline and post-RT samples collected within 6 months of RT. No men in the trial received adjuvant ADT and there was no difference in use of concurrent ADT between groups ($p = 0.861$). Of these 227 men, 40 had an increase in Hk2 post-treatment (defined as a rise above the pre-radiotherapy treatment value within 6 months of RT) (Fig 4a and Table 1) versus 187 who had no increase over baseline. These two groups were well balanced in regard to T-stage, Gleason score, and age. However, the 40 men with a rise in Hk2 post-EBRT showed trends of lower baseline total PSA, Free-PSA, and Free-Hk2 which would be expected to portend lower recurrence rates. In spite of these baseline differences that are associated with a favorable prognosis, the men with increased free-Hk2 levels post-EBRT experienced a greater than 3 fold increase in biochemical failure (median time from RT to biochemical failure of 32.9 months IQR [17.4 – 48.2]). Specifically, patients with an Hk2 gain versus those with no Hk2 gain had biochemical failure rates of 17.5% versus 5.3%, respectively (odds ratio 3.39 [95%CI 1.23–9.39], $p = 0.019$, Figure 4b). Furthermore, at 72 months post-treatment the patients without an Hk2 gain had significantly higher rates of freedom from PSA progression than those with an Hk2 gain (94.2% vs 83.5%, $p = 0.027$, Figure 4c). Importantly, Hk2 gain was defined very conservatively as it was not normalized to tumor shrinkage post-treatment. Because a considerable fraction of prostate cancer cells die during RT, one would expect overall serum Hk2 levels would decline post RT. Thus, an absolute rise in Hk2 post-therapy could represent a large increase in Hk2 protein expression on a per cell basis.

DISCUSSION

For decades the understanding of why the addition of ADT to RT improves survival has remained elusive (12–15). This question was further complicated by the knowledge that the addition of ADT to radical prostatectomy failed to improve survival (16). The recent discovery that ADT inhibits non-homologous end joining, a critical DNA repair process, provides a compelling answer to years of observed clinical trial outcomes (5–7). However, the new found clarity on this topic has subsequently created new questions. For instance, multiple randomized trials have demonstrated that the use of adjuvant ADT after combined ADT/RT also improves survival, but by unknown mechanisms (1,14). In contrast, a recently reported phase III trial tested whether an increase in the duration of ADT prior to the start of

RT would improve outcome, but failed to demonstrate a benefit for prolonged neoadjuvant ADT (3). These results suggest the timing of ADT in relationship to RT is perhaps more critical than simply the duration of use.

In the present report, we address the related issue of adjuvant ADT and provide mechanistic insight into why this clinical practice may be beneficial. Specifically, we show that RT induces upregulation of AR expression and activity across a panel of human prostate cancer cell lines and the magnitude of this upregulation is more strongly correlated with increased viability in a clonogenic survival assay than baseline AR expression. This association was confirmed in xenograft experiments, where LNCaP-AR tumors with the greatest percent increase in AR signaling post-RT showed more rapid time to progression. These preclinical findings appear to be relevant in patients, since we found that men experiencing an increase in serum hK2 levels post-RT were three times more likely to experience a biochemical failure than those with unchanged or declining hK2 post-treatment. Finally, we demonstrate that baseline AR and AR-output do not correlate with tumor response *in vitro*, *in vivo*, or in our patient serum data of hK2 levels.

Prior studies have reported that approximately 20% of men have increases in PSA during EBRT treatment (without the use of ADT), while the remainder had negatively sloping PSA declines (9). These results have previously been ignored due to the absence of evidence for clinical significance of inferior treatment outcomes (17). This clinical heterogeneity is also seen in our preclinical studies. One hypothesis that might explain the heterogeneity is variable amounts of hypoxia present in tumors, particularly since ADT has been shown to reduce prostate cancer hypoxia suggesting an interplay with AR-signaling (18,19). Our results suggest that AR activity during and after ADT/EBRT should be more closely studied with serum and imaging biomarkers to determine their prognostic significance. One potential implication is that adjuvant ADT may only be necessary for those men whose tumors upregulate AR as a response to RT. Alternatively, more potent AR inhibition using second generation ADT might prevent or mitigate the negative consequences of AR upregulation post-RT.

The underlying biological mechanism by which EBRT upregulates AR expression remains to be defined. Since AR mRNA levels are elevated in a dose dependent manner by EBRT, it is possible that a transcription factor that is sensitive to genotoxic stress elevates AR transcription. Potential candidates include Ku70 and Ku80, NFκB, and the STAT family (20–22). Ku is particularly promising given that the Ku70/Ku80 heterodimer recruits DNA-PKcs to double DNA strand breaks, and it has been demonstrated that both Ku70 and Ku80 directly interact with the ligand binding domain of the AR (22,23). In addition, the heterogeneity in magnitude and kinetics of RT-induced AR upregulation seen across *in vitro* and *in vivo* experiments is consistent with a stochastic variable that impacts RT response or a preexisting subset of tumor cells primed to respond to RT in this manner as an adaptive resistance mechanism. These critical points are areas for future investigation.

Supplementary Material

Refer to Web version on PubMed Central for supplementary material.

Acknowledgments

Financial Support: The Molecular Pharmacology & Chemistry Program Core (J.S. Lewis). The Radiological Society of North America 2013 Research Resident Grant #RR1350 (D.E. Spratt), the 2014 Rebecca and Nathan Milikowsky Prostate Cancer Foundation Young Investigator Award (D.E. Spratt), David H. Koch Young Investigator Award from the Prostate Cancer Foundation (M.J. Evans), the 2012 IMRAS MSKCC institutional grant (D.E. Spratt and M.J. Evans), NIH P50CA091956 MAYO CLINIC SPORE (D.J. Tindall, G.G. Klee and B.J. Davis), Grant from the T.J. Martell Foundation (D.J. Tindall), NIH P50CA09262 MSKCC SPORE (C.L. Sawyers) and the Howard Hughes Medical Institute (C.L. Sawyers).

We thank the Radiochemistry & Molecular Imaging Probe Core of MSKCC (P30 CA008748) for supply of the ^{18}F -FDHT and the MSKCC ICMIC. We also would like to thank both the MSKCC Prostate SPORE NIH P50CA09262, the Mayo Prostate SPORE NIH P50CA091956, and the Howard Hughes Medical Institute. DES and MJE are funded by Rebecca and Nathan Milikowsky and David H. Koch Young Investigator Awards from the Prostate Cancer Foundation, respectively, and we thank them for their support.

References

- Horwitz EM, Bae K, Hanks GE, Porter A, Grignon DJ, Brereton HD, et al. Ten-year follow-up of radiation therapy oncology group protocol 92-02: a phase III trial of the duration of elective androgen deprivation in locally advanced prostate cancer. *J Clin Oncol*. 2008; 26:2497-504. [PubMed: 18413638]
- Bolla M, De Reijke TM, Van Tienhoven G, Van den Bergh AC, Oddens J, Poortmans PM, et al. Duration of androgen suppression in the treatment of prostate cancer. *N Engl J Med*. 2009; 360:2516-27. [PubMed: 19516032]
- Pisansky TM, Hunt D, Gomella LG, Amin MB, Balogh AG, Chinn DM, et al. Duration of androgen suppression before radiotherapy for localized prostate cancer: Radiation Therapy Oncology Group randomized clinical trial 9910. *J Clin Oncol*. 2014; 58:0662.
- Alibhai SM, Gogov S, Alibhai Z. Long-term side effects of androgen deprivation therapy in men with non-metastatic prostate cancer: a systematic literature review. *Critical reviews in oncology/hematology*. 2006; 60:201-15. [PubMed: 16860998]
- Polkinghorn WR, Parker JS, Lee MX, Kass EM, Spratt DE, Iaquina PJ, et al. Androgen receptor signaling regulates DNA repair in prostate cancers. *Cancer discovery*. 2013; 3:1245-53. [PubMed: 24027196]
- Goodwin JF, Schiewer MJ, Dean JL, Schrecengost RS, de Leeuw R, Han S, et al. A hormone-DNA repair circuit governs the response to genotoxic insult. *Cancer discovery*. 2013; 3:1254-71. [PubMed: 24027197]
- Bartek J, Mistrik M, Bartkova J. Androgen Receptor Signaling Fuels DNA Repair and Radioresistance in Prostate Cancer. *Cancer discovery*. 2013; 3:1222-24. [PubMed: 24203954]
- Lawton CA, DeSilvio M, Roach M III, Uhl V, Kirsch R, Seider M, et al. An update of the phase III trial comparing whole pelvic to prostate only radiotherapy and neoadjuvant to adjuvant total androgen suppression: updated analysis of RTOG 94-13, with emphasis on unexpected hormone/radiation interactions. *IJROBP*. 2007; 69:646-55.
- Vijayakumar S, Quadri SF, Karrison T, Trinidad C, Chan S, Halpern H, et al. Localized prostate cancer: use of serial prostate-specific antigen measurements during radiation therapy. *Radiology*. 1992; 184:271-74. [PubMed: 1376933]
- Davis B, Klee G, Lieber M, Hillman D, Goodmanson M, Burch P, et al. Serum human glandular kallikrein 2 (HK2) concentration at presentation and early subsequent follow-up for patients undergoing primary radiotherapy or brachytherapy with or without androgen deprivation therapy for localized prostate cancer therapy. *IJROBP*. 2004; 60:S454.
- Klee GG, Goodmanson MK, Jacobsen SJ, Young CY, Finlay JA, Rittenhouse HG, et al. Highly sensitive automated chemiluminometric assay for measuring free human glandular kallikrein-2. *Clinical chemistry*. 1999; 45:800-06. [PubMed: 10351988]
- Jones CU, Hunt D, McGowan DG, Amin MB, Chetner MP, Bruner DW, et al. Radiotherapy and short-term androgen deprivation for localized prostate cancer. *N Engl J Med*. 2011; 365:107-18. [PubMed: 21751904]

13. Roach M, Bae K, Speight J, Wolkov HB, Rubin P, Lee RJ, et al. Short-term neoadjuvant androgen deprivation therapy and external-beam radiotherapy for locally advanced prostate cancer: long-term results of RTOG 8610. *J Clin Oncol*. 2008; 26:585–91. [PubMed: 18172188]
14. Bolla M, Van Tienhoven G, Warde P, Dubois JB, Mirimanoff R-O, Storme G, et al. External irradiation with or without long-term androgen suppression for prostate cancer with high metastatic risk: 10-year results of an EORTC randomised study. *Lancet oncology*. 2010; 11:1066–73. [PubMed: 20933466]
15. Jones CU, Hunt D, McGowan DG, Amin MB, Chetner MP, Bruner DW, et al. Radiotherapy and short-term androgen deprivation for localized prostate cancer. *N Engl J Med*. 2011; 365:107–18. [PubMed: 21751904]
16. Shelley M, Kumar S, Wilt T, Staffurth J, Coles B, Mason M. A systematic review and meta-analysis of randomised trials of neo-adjuvant hormone therapy for localised and locally advanced prostate carcinoma. *Cancer treatment reviews*. 2009; 35:9–17. [PubMed: 18926640]
17. Halperin, EC.; Brady, LW.; Wazer, DE.; Perez, CA. *Perez & Brady's Principles and Practice of Radiation Oncology*. Lippincott Williams & Wilkins; 2013.
18. Milosevic M, Chung P, Parker C, Bristow R, Toi A, Panzarella T, et al. Androgen withdrawal in patients reduces prostate cancer hypoxia: implications for disease progression and radiation response. *Cancer research*. 2007; 67:6022–25. [PubMed: 17616657]
19. Milosevic M, Warde P, Ménard C, Chung P, Toi A, Ishkanian A, et al. Tumor hypoxia predicts biochemical failure following radiotherapy for clinically localized prostate cancer. *Clinical Cancer Research*. 2012; 18:2108–14. [PubMed: 22465832]
20. Veuger SJ, Hunter JE, Durkacz BW. Ionizing radiation-induced NF- κ B activation requires PARP-1 function to confer radioresistance. *Oncogene*. 2008; 28:832–42. [PubMed: 19060926]
21. Mills IG. Maintaining and reprogramming genomic androgen receptor activity in prostate cancer. *Nature Reviews Cancer*. 2014; 14:187–98. [PubMed: 24561445]
22. Mayeur GL, Kung W-J, Martinez A, Izumiya C, Chen DJ, Kung H-J. Ku is a novel transcriptional recycling coactivator of the androgen receptor in prostate cancer cells. *Journal of Biological Chemistry*. 2005; 280:10827–33. [PubMed: 15640154]
23. Spagnolo L, Rivera-Calzada A, Pearl LH, Llorca O. Three-dimensional structure of the human DNA-PKcs/Ku70/Ku80 complex assembled on DNA and its implications for DNA DSB repair. *Molecular cell*. 2006; 22:511–19. [PubMed: 16713581]

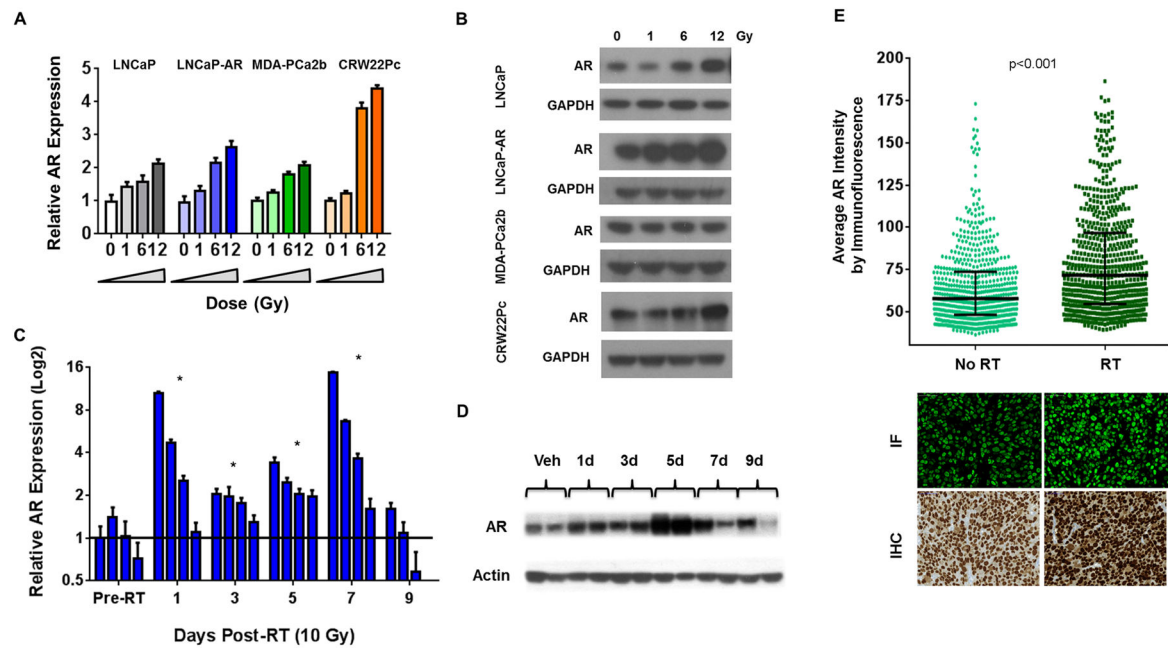


Figure 1. RT induces increased expression of the androgen receptor

(A) LNCaP, LNCaP-AR, MDA-PCa2b, and CRW22Pc cell lines were treated with either 0, 1, 6, or 12 Gy or EBRT and the cells harvested for mRNA measured by qPCR, and (B) protein by western blot.

(C) LNCaP-AR derived xenografts were treated with 10 Gy of conformal EBRT and compared to non-irradiated controls, and mRNA for AR was measured by qPCR, and (D) protein by western blot.

(E) LNCaP-AR xenografts were treated with 10 Gy of EBRT and harvested 5 days after treatment, fixed and formalin and paraffin embedded and stained by IHC and immunofluorescence for AR.

Significance level indicated by * ($p < 0.05$) or p-value listed in figure.

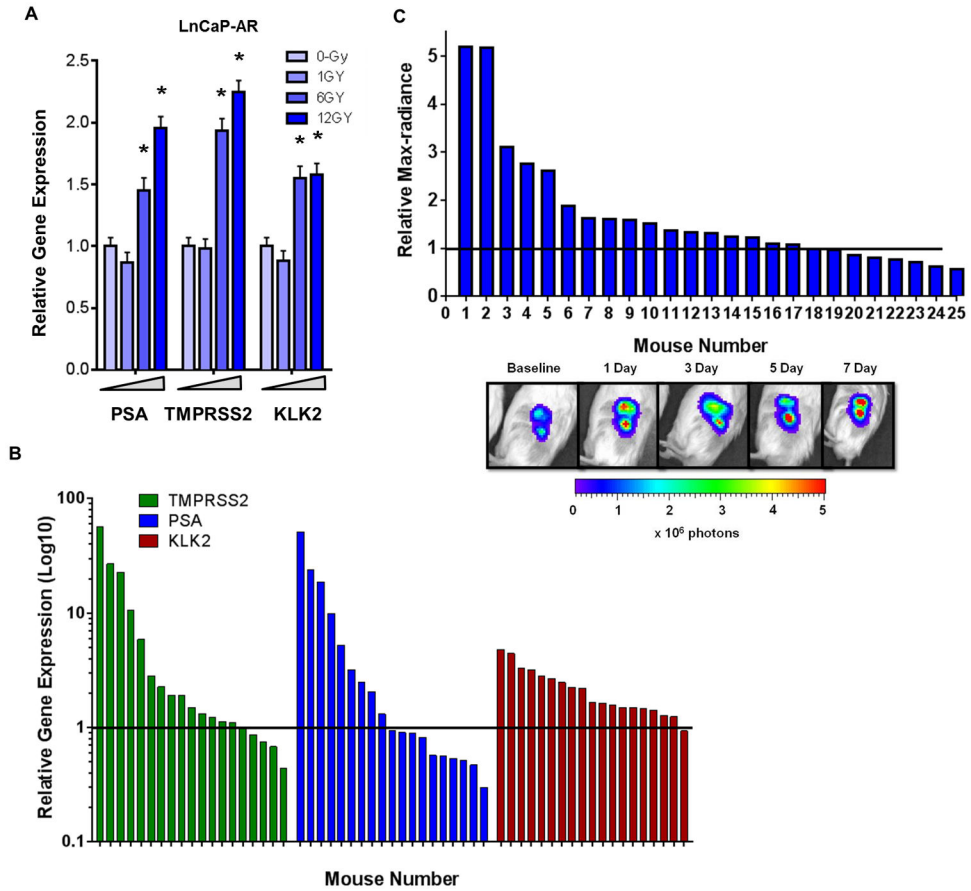


Figure 2. AR transcriptional output is increased following RT

(A) LNCaP-AR *in vitro* qPCR assessment of AR target genes PSA, TMPRSS2, and KLK2 mRNA expression post-EBRT (0, 1, 6, 12 Gy).

(B) LNCaP-AR xenografts irradiated with 10 Gy and harvested over the first week post-RT and mRNA by qPCR was analyzed for the AR target genes TMPRSS2, PSA, and KLK2.

(C) Bioluminescence assay of 25 SCID mice with LNCaP-AR xenografts imaged at baseline and then treated with 10 Gy of conformal EBRT. Subsequent imaging performed during the first week post-RT and the max increase in bioluminescence was recorded. The bottom panel demonstrates the acute and persistent increase in AR-output measured by bioluminescence from mouse #1 in the companion graph.

Significance level indicated by * ($p < 0.05$) or p-value listed in figure.

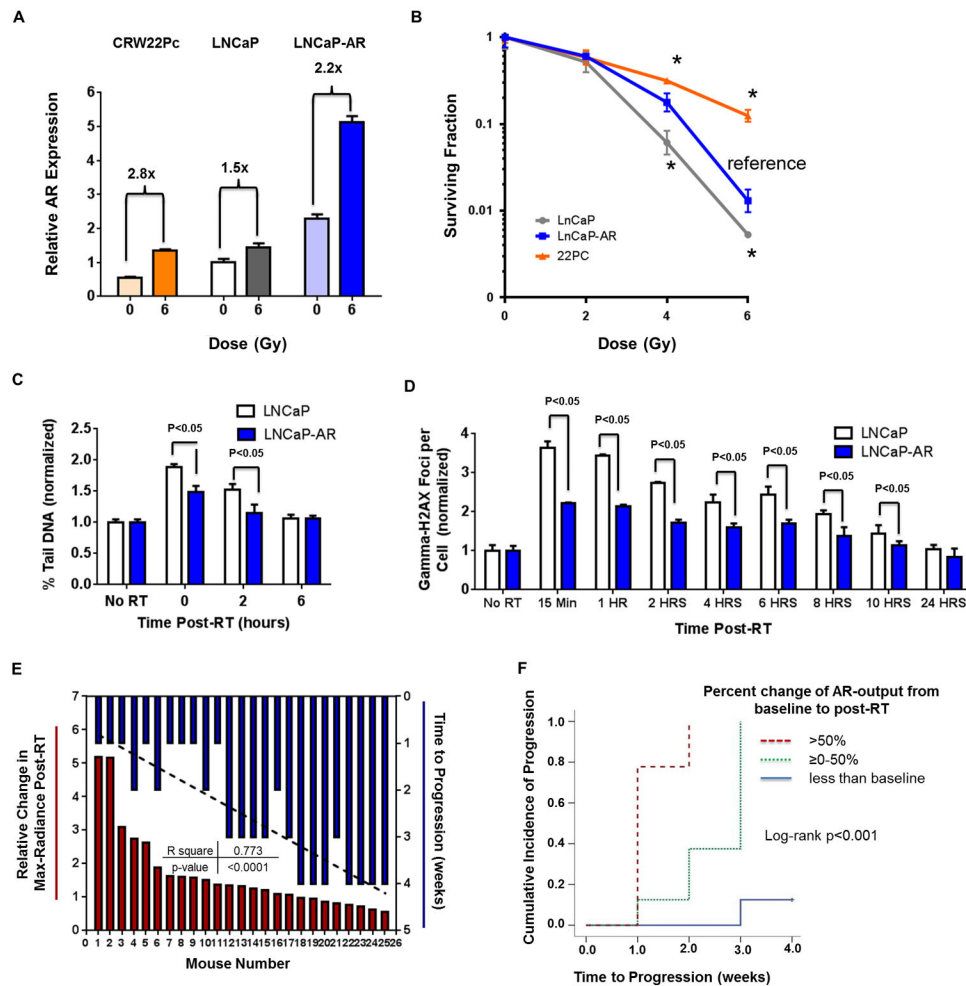


Figure 3. Increased AR signaling post-RT correlates with increased DNA repair and cancer cell survival

(A) Relative upregulation of AR mRNA after 6 Gy of EBRT in CWR22Pc, LNCaP, and LNCaP-AR cell lines. 22Pc cells had the greatest AR induction despite having the lowest baseline AR expression level.

(B) Long-term clonogenic survival assay comparing cell lines with different baseline AR expression and different magnitudes of AR induction.

(C) Neutral comet assay and (D) gamma-H2AX immunofluorescence were performed to compare LNCaP and LNCaP-AR cells after 6 Gy of EBRT.

(E) Waterfall plot of AR-output upregulation post-RT measured by max-radiance from *in vivo* bioluminescence of LNCaP-AR tumors (red) co-plotted with time to tumor progression (blue) (R^2 0.77, $p < 0.001$).

(F) Cumulative incidence of mice categorically subgrouped into three groups from panel D (>50%, 0–50%, <0% increase in bioluminescence).

Significance level indicated by * ($p < 0.05$) or p-value listed in figure.

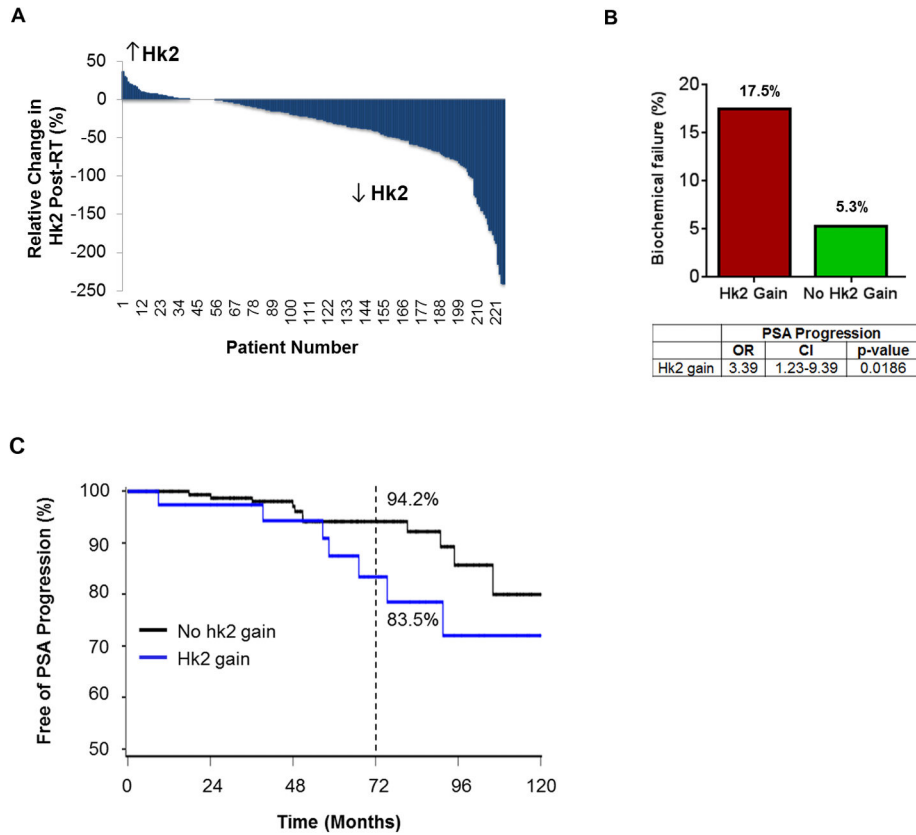


Figure 4. Serum hK2 up-regulation post-RT is associated with biochemical failure in 227 men treated with definitive EBRT for localized prostate cancer

A. Waterfall plot of percent change in hK2 post-RT compared to baseline.

B. Comparison of biochemical relapse outcomes in men who had an hK2 gain post-RT (n=40) versus those who did not (n=187); (odds ratio 3.39 [95% CI 1.23–9.39], p=0.019).

C. Kaplan-Meier curves for Freedom of PSA progression by Hk2 gain status. Estimates at 72 months for Hk2 gain were 83.5% compared to 94.2% for those without an Hk2 gain (p=0.027).

Table 1

Baseline characteristics of patients by Hk2 gain status.

	Cohort Summary by Hk2 gain			p value
	Total (N=227)	No Hk2 Increase (N=187)	Hk2 Increase (N=40)	
Race				1.0000 ^A
Missing	1	1	0	
Asian	1 (0.4%)	1 (0.5%)	0 (0.0%)	
White	225 (99.6%)	185 (99.5%)	40 (100.0%)	
Age at Baseline				0.6933 ^B
N	227	187	40	
Mean (SD)	68.5 (7.0)	68.6 (6.8)	67.9 (7.7)	
Median	70.0	69.0	70.0	
Q1, Q3	64.0, 74.0	64.0, 74.0	64.0, 73.0	
Baseline Serum PSA				0.0001 ^B
N	227	187	40	
Mean (SD)	6.2 (6.6)	6.7 (6.8)	3.7 (5.1)	
Median	5.6	6.0	1.3	
Q1, Q3	1.7, 8.8	2.7, 9.1	0.2, 4.8	
Baseline Serum-Free PSA				<0.0001 ^B
N	227	187	40	
Mean (SD)	0.9 (0.9)	0.9 (0.8)	0.6 (1.1)	
Median	0.7	0.8	0.2	
Q1, Q3	0.2, 1.2	0.4, 1.3	0.1, 0.7	
Baseline Serum-Free HK2				<0.0001 ^B
N	227	187	40	
Mean (SD)	56.3 (76.7)	65.2 (81.5)	14.4 (16.4)	
Median	41.0	49.0	9.0	
Q1, Q3	13.0, 74.0	22.0, 79.0	3.9, 19.0	
Clinical T stage				1.0000 ^A
Missing	1	1	0	
T1	134 (59.3%)	110 (59.1%)	24 (60.0%)	
T2	88 (38.9%)	73 (39.2%)	15 (37.5%)	
T3/T4	4 (1.8%)	3 (1.6%)	1 (2.5%)	
Gleason Group				0.8789 ^C
≤6	148 (65.2%)	122 (65.2%)	26 (65.0%)	
7	70 (30.8%)	58 (31.0%)	12 (30.0%)	
≥8	9 (4.0%)	7 (3.7%)	2 (5.0%)	

^A Fisher's Exact Test^B Wilcoxon-Mann-Whitney Test^C Mantel-Haenszel Chi-Square Test